J Membrane Biol (2011) 242:153–164
DOI 10.1007/s00232-011-9386-2

Identification of a Novel Bacterial K^+ Channel

Guanghua Tang · Bo Jiang · Yuan Huang · Ming Fu · Lingyun Wu · Rui Wang

Received: 4 May 2011 / Accepted: 27 June 2011 / Published online: 9 July 2011

Abstract In an attempt to explore unknown K^+ channels in mammalian cells, especially ATP-sensitive K^+ (K_{ATP}) channels, we compared the sequence homology of Kir6.1 and Kir6.2, two pore-forming subunits of mammalian K_{ATP} channel genes, with bacterial genes that code for selective proteins with confirmed or putative ion transport properties. BLAST analysis revealed that a prokaryotic gene (*ydfJ*) expressed in *Escherichia coli* K12 strain shared 8.6% homology with Kir6.1 and 8.3% with Kir6.2 genes. Subsequently, we cloned and sequenced *ydfJ* gene from *E. coli* K12 and heterologously expressed it in mammalian HEK-293 cells. The whole-cell patch-clamp technique was used to record ion channel currents generated by *ydfJ*-encoded protein. Heterologous expression of *ydfJ* gene in HEK-293 cells yielded a novel K^+ channel current that was inwardly rectified and had a reversal potential close to K^+ equilibrium potential. The expressed *ydfJ* channel was blocked reversibly by low concentration of barium in a dose-dependent fashion. Specific K_{ATP} channel openers or blockers did not alter the K^+ current generated by *ydfJ* expression alone or *ydfJ* coexpressed with rvSUR1 or rvSUR2B subunits of K_{ATP} channel complex. Furthermore, this coexpressed *ydfJ*/rvSUR1 channels were not inhibited by ATP dialysis. On the other hand, *ydfJ* K^+ currents were inhibited by protopine (a nonspecific K^+ channel blocker) but not by dofetilide (a HERG channel blocker). In summary, heterologously expressed prokaryotic *ydfJ* gene formed a novel functional K^+ channel in mammalian cells.

Keywords Bacteria · *E. coli* · HEK-293 · K^+ channel · Kir6.1 · Protopine · Transfection · *ydfJ* gene

Inwardly rectifying K^+ (Kir) channels are distributed widely in different types of cells and tissues and play important roles in controlling the resting membrane potential and various K^+ transport processes (Bichet et al. 2003; Reimann and Ashcroft 1999). Human genome contains 15 different Kir channel genes within 7 subfamilies (KCNJ1-7) (Reimann and Ashcroft 1999). Mutations of Kir channel genes cause various disorders and diseases such as congenital hyperinsulinemia, neonatal diabetes, Andersen's syndrome, and Bartter's syndrome (Ashcroft 2005; Hebert 2003; Plaster et al. 2001). Selective types of Kir channels, e.g., Kir6.x including Kir6.1 and Kir6.2, constitute the pore-forming subunits of K_{ATP} channels, which link metabolic activity and membrane excitability and protection cells against ischemic insults and oxidative stress (Seino 1999; Ashcroft 2005). In addition to Kir6.x, K_{ATP} channel complex also include regulatory sulfonylurea receptors (SURs). Our knowledge on the complexity of Kir channels in mammalian cells is incomplete, and the molecular composition of many different subfamilies of Kir channels is still waiting to be elucidated.

Electronic supplementary material The online version of this article (doi:10.1007/s00232-011-9386-2) contains supplementary material, which is available to authorized users.

G. Tang · R. Wang
Department of Physiology and Pathophysiology, Fudan University, Shanghai, People's Republic of China

G. Tang · B. Jiang · Y. Huang · L. Wu
Department of Pharmacology, University of Saskatchewan, Saskatoon, SK, Canada

M. Fu · R. Wang (✉)
Department of Biology, Lakehead University, 955 Oliver Road, Thunder Bay, ON P7B 5E1, Canada
e-mail: rwang@lakeheadu.ca

Ion transport machineries are widely expressed and conserved in all known phylogenetic domains of life, including bacteria, archaea, and eukarya. Advance in sequencing bacterial genomes reveals that ion channels may evolve as early as three billion years ago. Efforts have been made to analyze prokaryotic homologs of mammalian ion channels (Kowalski and Martinac 2005; Kuo et al. 2005a, b; Kung and Blount 2004). Analysis of evolutionary relationships between bacterial ion transport proteins and the conserved sequence of mammalian Kir channels may aid in resolving molecular composition of certain unknown Kir channels (Durell and Guy 2001). To date, there has been no report on heterologous expression of bacterial channel genes in eukaryotic cells, although purified prokaryotic Kir channel proteins have been reconstituted in liposomes (Enkvetchakul et al. 2005a, b; Cheng et al. 2009) or in artificial lipid bilayers (Jiang et al. 2002; Ruta et al. 2003). Furthermore, the molecular structure of mitochondrial K_{ATP} channels is also waited to be elucidated because mitochondria are evolved from bacteria. Therefore, the comparison of bacterial genomes with sarcolemma Kir gene sequences would provide clues for the possible structures of mitochondrial K_{ATP} channels.

In the present study, we searched available bacterial genomes for clues for unknown K^+ channels, especially Kir6.1- and Kir6.2-like channels. This homologs search led to the cloning and sequencing of a bacterial *ydfJ* gene from *Escherichia coli* K12, which likely encodes an ion transport protein (Dobrindt 2005; Blattner et al. 1997). The whole-cell patch clamp technique was used to characterize the K^+ currents generated by *ydfJ* gene transfected in HEK-293 cells. This study demonstrated that heterologously expressed prokaryotic *ydfJ* gene formed a novel functional K^+ channel in mammalian cells.

Materials and Methods

Bioinformatic Analysis

Available bacterial genomic DNA sequences were downloaded from the National center for Biotechnology information (NCBI) GenBank at http://ncbi.nlm.nih.gov/genbanl/genomes, and sequence homology searches were performed with the web-based program Psi-Blast available at http://ncbi.nlm.nih.gov/microbj3blast/genbanl/genomes. The amino acid sequences of K^+ selectivity filters were aligned using the Clustal W 2.0 multiple-alignment program (Higgins and Sharp 1988). To search for gene bank (NCBI homepage) by using the reserved transmembrane (TM1, TM2) domains and GFG motif in pore-forming region of Kir subunits of K_{ATP} channels (Blattner et al. 1997; Seino 1999), *E. coli* K12 bacterial genes were screened and three candidate genes (*ybbW*, *ydeE*, and *ydfJ* with NCBI reference sequence number of NP_415044, NP_416051, NP_416061, respectively) were selected with both conserved motifs in TM2 and GFG motif (Supplemental Tables 1, 2).

Amplification, Cloning, and Sequencing of K^+ Channel-related Genes in *E. coli* K12

Escherichia coli K12 genome (GenBank U00096) was kindly provided as a gift from Dr. Ganetzky (University of Wisconsin, Madison, WI, USA). The open reading frames of the selected candidate K^+ channel-related genes were amplified with 35 cycles. Each PCR cycle was composed of 94°C for 2 min, followed by 94°C for 30 s, 58°C for 30 s, and 68°C for 45 s. The PCR products were generated by using specific designed primers: *ybbW:* forward primer: 5′-AATTATGTGATGGT CGGCGG-3′, reverse primer: 5′-TTCAATATCGGG ATTAATTA-3′; *ydfJ:* forward primer: 5′-CTGTGAATTATGGATTTCCA-3′, reverse primer: 5′-TAAGGG TTTACAGACTTCTG-3′; *ydeE:* forward primer: 5′-CAAATGAACTTATCC CTACG-3′, reverse primer: 5′-TTCGACTTAAATCAACAAAG-3′. The amplified PCR products were identified on agarose gel staining with ethidium bromide.

Three PCR products were gel purified using a MinElution PCR purification kit (Qiagen). After purification, they were inserted into a TA cloning pCR 3.1 vector with ligase. The constructs containing pCR3.1-*ydfJ* cDNA clones were cleaved with *Nhe*I and *Hin*dIII and *ydfJ* gene was cloned into *Nhe*I–*Hin*dIII site of pcDNA3.1/Hygromycin vector (Invitrogen). These plasmids were transformed into *E. coli* competent cells in Luria broth (LB) plates containing 100 μg/ml ampicillin. Recombinant clones were identified as colorless colonies and picked up for further overnight culturing in LB broth culture media containing ampicillin. The culture media were collected and plasmid DNA was extracted using a miniprep kit (Qiagen). The insertion of bacterial gene was confirmed with both Bam HI endonuclease and DNA sequencing (ABI 373A, Applied Biosystem).

Transfection of HEK-293 Cells with *ydfJ* Alone or Together with SURx

HEK-293 cells (CRL 1573, batch 203970) were obtained from the American Type Culture Collection (ATCC) (Rockville, MD, USA) and cultured at 37°C in a humidified atmosphere containing 5% CO_2/95% air. RPMI-1640 medium (Sigma) was used with supplementation of 10% fetal bovine serum and penicillin 100 U/ml. The culture medium was changed every 3 days.

ydfJ gene was cloned into pcDNA3.1/Hygromycin vector (Invitrogen) for stable transfection; while rvSUR2B

or rvSUR1 (rv stands for rat vascular) genes were prepared to cloned into pIRES2-EGFP vectors (Clontech) for transiently transfection as described before in our previous publication (Cao et al. 2002). All DNA plasmid transfections were performed using Fugene 6 (Roche Applied Science) according to the manufacturer's instructions. Mock transfection (pcDNA3.1/ pIRES2-EGFP vector only) was also performed. Nontransfected HEK-293 cells were included as negative control for antibiotic selection.

For stable transfection, the constructs containing *ydfJ*-pcDNA3.1 were linearized with Eam1105I restriction endonuclease (MBI Fermentas). Linearized constructs were mixed with a FUGENE 6 transfection reagent (Roche) in a ratio of 1:3 (μg/μl) in 100 μl of FBS-free RPMI-1640 medium. After incubation for 45 min at room temperature (20–22°C), the mixture was added to HEK-293 cells in 2 ml FBS-free RPMI-1640 medium. The hygromycin (80 μg/ml) was added in the culture media and cultured for about 10 days until hygromycin resistant cell strains formed. Then these antibiotic resistant cell strains were picked individually into a 12-well culture plate for proliferation and continue to culture under the same antibiotic pressure. When these cells became >90% confluent, they were harvested and stored. The expression of *ydfJ*-pcDNA3.1 was confirmed with RT-PCR as described previously (Cao et al. 2002). For transient transfection, constructs containing pIRES2-EGFP-rvSUR2B or -rvSUR1 cDNA were used to transiently transfect *ydfJ*-pcDNA3.1 stably transfected HEK-293 cell line using Fugene 6. pIRES2-EGFP vector encodes a green fluorescent protein (GFP) for easy identification of transfected cells. Cells were allowed to express rvSUR2B and rvSUR1 for 48–72 h before electrophysiological experiments.

Recording of Expressed K^+ Channel Currents

Whole-cell K^+ channel currents in HEK-293 cells transfected with *ydfJ* alone or cotransfected with *ydfJ*/SURx were measured using the whole-cell configuration of the patch-clamp technique as described previously (Tang et al. 2005; Cao et al. 2002). Briefly, 35 mm petri dishes with the attached cells were mounted on the stage of an inverted phase contrast microscope (Olympus IX70). A homemade superfusion chamber was inserted into the petri dish. In all experiments the cells inside the chamber (volume of 1 ml) were superfused continuously at a flow rate of 3–5 ml/min. The time required for a complete solution change from the onset of a drug application was estimated at 10–15 s, as described before. Pipettes were pulled from soft microhematocrit capillary tubes (Fisher, Nepean, ON) with tip resistance of 2–4 MΩ when filled with the pipette solution. Currents were recorded with an Axopatch 200-B amplifier (Molecular Device), controlled by a Digidata 1200 interface and a pCLAMP software (Version 6.02, Molecular Device). Membrane currents were filtered at 1 kHz with a four-pole Bessel filter. At the beginning of each experiment, junction potential was electronically adjusted to zero. Leakage subtractions were not routinely performed on the original current records. Current–voltage curves were constructed using the sustained current amplitude at the end of different depolarization steps.

Unless otherwise specified, the bath solution contained (mM) 140 NaCl, 5.4 KCl, 1.2 $MgCl_2$, 1 $CaCl_2$, 10 HEPES, and 5 glucose (pH adjusted to 7.3 with NaOH) (Wu et al. 2002). Because HEPES was chosen as a pH buffer (for the range between 6.8 and 8.3), the pH value of bath solution was kept in alkaline solution adjusted by NaOH, minimizing the activation of acid-sensitive ion channels and transporters. When the concentration of KCl of the bath solution was altered in some experiments, it was replaced by equimolar concentration of NaCl to maintain the osmolality unaltered. The pipette solution contained (mM): 110 KCl, 30 KOH, 1 $MgCl_2$, 1 EGTA, 10 HEPES, and 0.3 Na_2-ATP (pH adjusted to 7.3 with KOH). Low concentration of ATP in the pipette solution is critical to keep K_{ATP} channel activity, reduce the run-down of the channel currents, and maintain the cellular energy source (Jiang et al. 2004, 2010). Test pulses were applied in a stepwise fashion with an interval of 10 s in 10 mV increments from −150 mV to +80 mV. Unless otherwise specified, the holding potential was set at −80 mV. To amplify the inward K^+ currents, membrane currents were measured by holding membrane potential at −60 mV with symmetric 140 mM $[K^+]_o$. The reversal potential of transmembrane current was measured from either I–V curves or classic instantaneous tail current. The latter is used for tiny inward currents in 5.4 mM $[K^+]_o$, especially in Mock-transfected cells. The resting membrane conductance was determined using linear regression across the linear part (−60 to −80 mV) of the current–voltage (I–V) plot obtained using voltage step pulses of varying amplitude (−150 to −50 mV from the holding potential of −80 mV for 1-s duration). All experiments were conducted at room temperature (20–22°C). The osmolarity of recording solutions was always adjusted to 300 mOsms.

Results

Identification and Cloning of Kir Channel-related Genes in *E. coli* K12

Mammalian Kir channel subunits consist of two conserved transmembrane helices (TM1 and TM2) bridged by an extracellular pore loop (H5) that contains the signature K^+ selectivity sequence: Gly-Phe-Gly (GFG) motifs

(Loussouarn et al. 2002). On the basis of known cDNA sequences of TM1–H5–TM2 of rvKir6.1/rvKir6.2 genes, 148 bacterial genome sequences in GenBank were searched by BLAST (Seino 1999). Among them, 22 genes were identified to contain the reserved TM1 and TM2 domains and GFG motifs in the putative pore-forming region common to Kir6.x. These 22 genes are distributed in 12 bacteria such as *E. coli* K12, *Yersinia pestis* KIM, and *Streptomyces coelicolor* A3(2) (Supplemental Tables 1, 2). Amino acid sequences between the identified 22 bacterial gene products and rvKir6.1/rvKir6.2 are compared (Supplemental Tables 1, 2) and multiple alignment of the amino acid sequence of the conserved region in *ydfJ,* rvKir6.1, and rvKir6.2 are shown in Table 1. None of the 22 bacterial gene products possessed the exact TM1–H5–TM2 amino acid sequence as for rvKir6.1/rvKir6.2. The top three bacteria, whose gene products are with the highest percent identity to conserved functional TM1–H5–TM2 region of rvKir6.1/rvKir6.2, are *Y. pestis* KIM, *E. coli* K12, and *S. coelicolor* A3(2). Each of three bacterial strains has multiple gene products with similar conserved sequence to rvKir6.1/rvKir6.2. For example, three gene products (*ydfJ, ydeE,* and *ybbW*) from *E. coli* K12 have 8.6, 7.4, and 7.1%, respectively, with the average of 7.7% homogeneity with Kir6.1 (Supplemental Table 1); whereas they have 8.3, 9.1, and 8.8%, respectively, with the average of 8.7% homogeneity with Kir6.2 Supplemental Table 2). Five gene products from *Y. pestis* KIM have the average of 9.1% homogeneity to Kir6.1 and 8.1% to Kir6.2 (Supplemental Tables 1, 2). Three gene products from *S. coelicolor* A3(2) have the average homogeneity of 7.5% to Kir6.1 and 9.6% to Kir6.2 (Supplemental Tables 1, 2). On the basis of the availability of bacterial strains in the lab and the homogeneity degree of the selected bacterial gene sequences with that of the signature tripeptide GFG and TM motifs that are common to rvKir6.1/rvKir6.2, *E. coli* K12 strain was chosen as a candidate bacterial species in the present study.

From *E. coli* K12 strains, three genes were identified with relative high degree of homogeneity of gene sequence with that of rvKir6.1/rvKir6.2 and contained different INA/MLGCI/QNIVGL motifs in TM2 domain and GFG motif of pore-forming H5 region (Supplemental Table 3). PCR was conducted on *E. coli* K12 genomic DNA to amplify *ybbW*, *ydeE*, and *ydfJ* genes. The coding regions of three genes were amplified as 1340-, 1202-, and 1300-bp fragments for *ybbW*, *ydeE*, and *ydfJ,* respectively (Fig. 1a).

Table 1 Multiple alignment of amino acid sequences of *ydfJ* with the conserved region of Kir6.1, Kir6.2, and KirBac1.1 channels

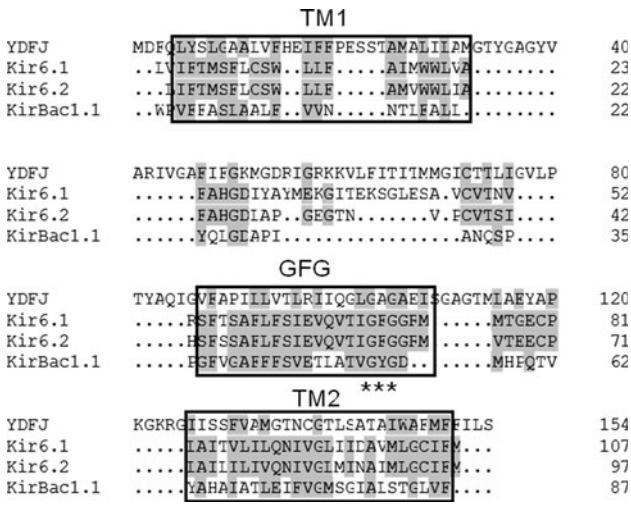

The aligned amino acid sequences with more than 50% matching the consensus sequence are shaded. Functionally important amino acids are indicated by asterisks. Gaps introduced to generate this alignment are represented by dots. *ydfJ,* Kir6.1 (*Rattus norvegicus*, GenBank BAA96237), Kir6.2 (*Rattus norvegicus*, GenBank BAA96239), KirBac1.1 (*Burkholderia pseudomallei*, GenBank 1P7B_B)

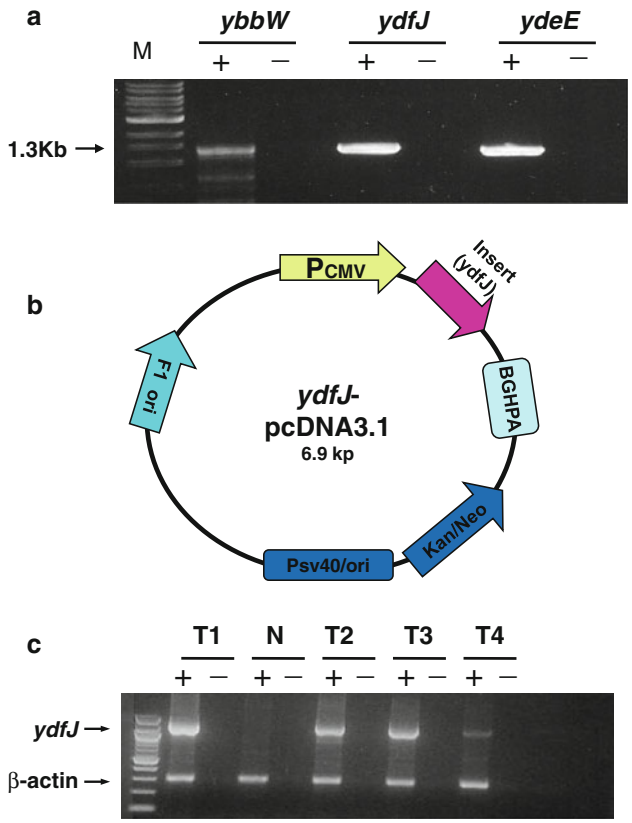

Fig. 1 Screening of K^+ channel-related genes in *E. coli* K12 and cloning and transfection of *ydfJ* gene into HEK-293 cells. **a** PCR amplification of coding region of three *E. coli* K12 genes using gene specific primers. *M* molecular marker; + RT plus samples, − RT minus samples. **b** Insertion of purified *ydfJ* PCR product to pcDNA3.1 eukaryotic expression vector using a TA cloning kit. **c** RT-PCR analyses of *ydfJ* clones transfected into HEK-293 cells. *M* molecular marker, *N* nontransfected HEK-293 cells, *T1–4* *ydfJ*-transfected HEK-293 cells

Among three genes, *ydfJ* has the highest percentage of homogeneity (8.6%) of amino acid sequence with rvKir6.1 (Supplemental Table 1), and a lesser homogeneity (8.3%) with rvKir6.2 (Supplemental Table 2). Therefore, the *ydfJ* gene was chosen for further functional expression study. In order to confirm *ydfJ* clone sequence, we ligated *ydfJ* DNA to pCR3.1 vectors and transformed them into *E. coli* competent cells. Recombinant clones were identified by sequencing. Total 13 colonies that expressed *ydfJ* genes were collected and proliferated. Purified *ydfJ*-pCR3.1 vectors (Fig. 1b) from these 13 bacterial colonies were used to transfect HEK-293 cells. RT-PCR confirmed the expression of *ydfJ* gene in permanently transfected HEK-293 cells compared with nontransfected HEK-293 cells (Fig. 1c).

Characterization of Heterologously Expressed *ydfJ* Channels

There was no evident morphological change of the transfected cells with *ydfJ* compared with nontransfected HEK-293 cells and no viability change occurred in stably transfected cells with *ydfJ* or transiently transfected cells with SURx (data not shown). The heterologous expression of *ydfJ* genes, obtained from all 13 bacterial colonies, yielded novel transmembrane currents in HEK-293 cells. Among total 13 colonies, transmembrane currents generated by *ydfJ* gene were examined from five colonies (BH3b, 5b, 7b, 9b, 10b) at different $[K^+]_o$ and other eight colonies (HB2, 3, 4, 5, 7, 13, 14, 15) at different HP. In BH colonies, I_K-in dramatically amplified ($n = 8$, $P < 0.01$) and I_K-out significantly suppressed ($n = 8$, $P < 0.01$) when $[K^+]_o$ was elevated from 5.4 to 40 mM with the same HP of −80 mV (Fig. 2a, b). In HB colonies, switch of HP from −80 to −30 mV did not change I_K-in ($n = 9$) but decreased I_K-out ($n = 9$, $P < 0.05$) (Fig. 2c, d). Because *ydfJ* cDNA obtained from bacterial colony HB7 produced the greatest current in transfected cells, this cDNA from colony HB7 was used in all following electrophysiological and pharmacological studies.

To differentiate native K^+ currents in HEK-293 cells from heterologously expressed *ydfJ* K^+ currents, total transmembrane K^+ currents, including outward (I_K-out) and inward (I_K-in) currents, were compared between mock-transfected and *ydfJ* transfected cells (Fig. 3). We used HEK-293 cells at the passage of 35–38 for the gene transfection. The average capacitance for each group is 14.8 ± 1.7 pF ($n = 31$) for HEK-293 cells without

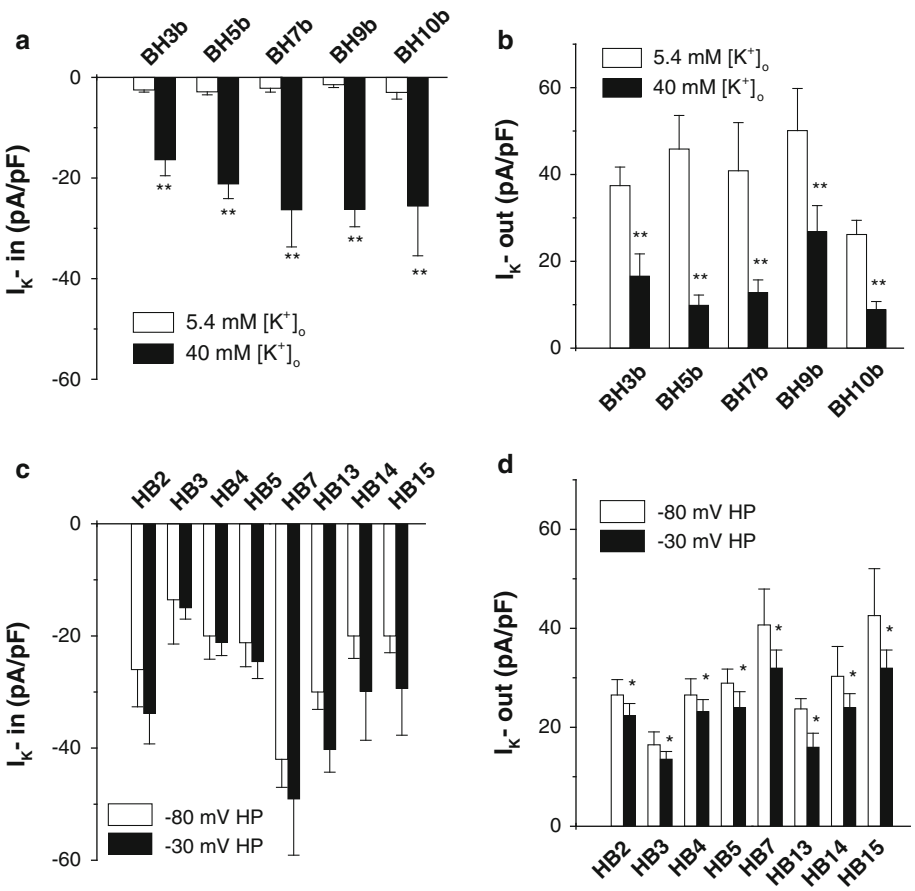

Fig. 2 Transmembrane currents in transfected HEK-293 cells with *ydfJ* gene from 13 *E. coli* K12 colonies. **a** Summary of inward K^+ currents (I_K-in) from five bacterial colonies at different $[K^+]_o$. Testing potential (TP) at −100 mV; Holding potentials (HP) at −80 mV ($n = 9$). $^{**}P < 0.01$. **b** Summary of outward K^+ currents (I_K-out) from the same five colonies as in (**a**). TP = +50 mV; HP = −80 mV ($n = 9$). $^{**}P < 0.01$. **c** Summary of I_K-in currents with 40 mM $[K^+]_o$ from eight colonies at different HP. TP = −100 mV ($n = 8$). **d** Summary of I_K-out currents with 40 mM $[K^+]_o$ from the same eight colonies at different HP. TP = +50 mV ($n = 8$). $^{*}P < 0.05$

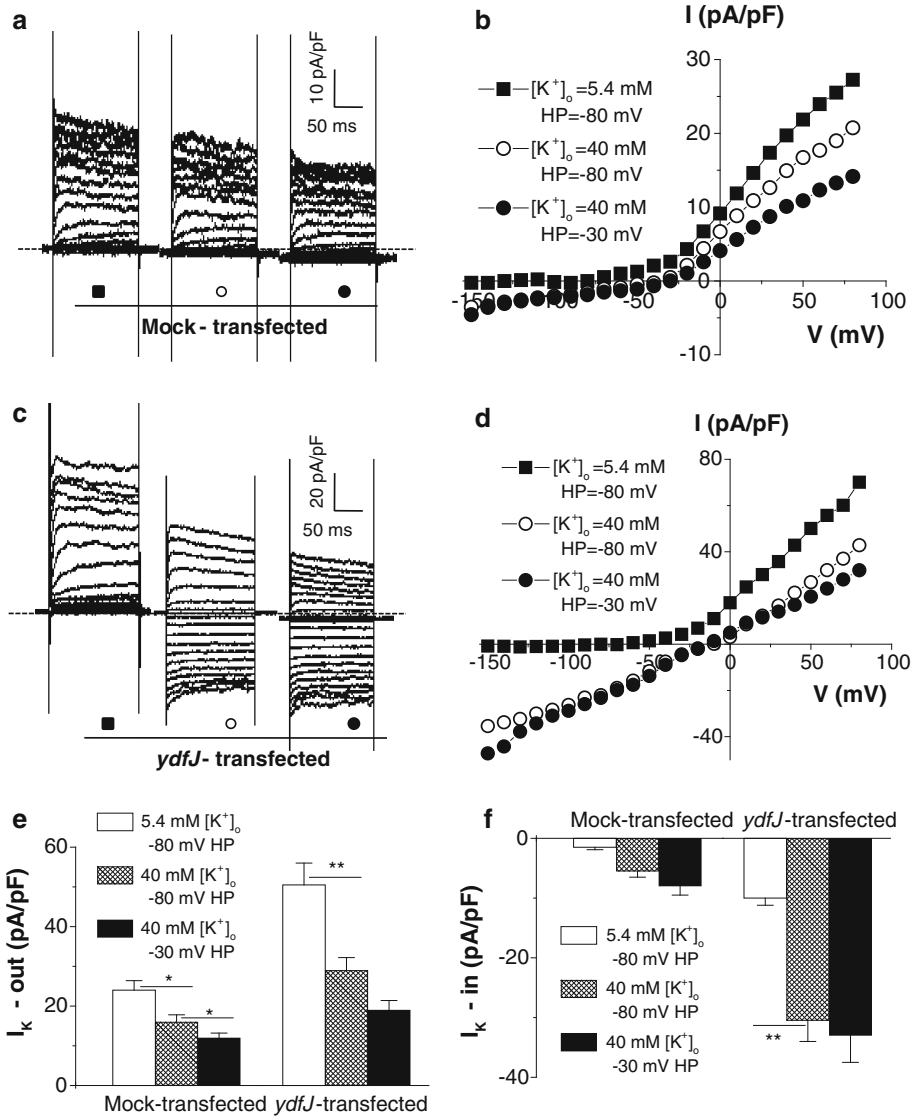

Fig. 3 K^+ currents recorded in mock-transfected cells and *ydfJ* gene-transfected HEK-293 cells. **a** Original K^+ current traces in mock-transfected cells at different holding potential (HP, −30 mV and −80 mV) and $[K^+]_o$ (5.4 and 40 mM). **b** The I–V relationships of the transmembrane currents obtained from the same cell in (**a**). **c** Original K^+ current traces in *ydfJ* gene-transfected cells at different HP and $[K^+]_o$. **d** The I–V relationship curves obtained from the same cell as in (**c**). **e** Summary of outward K^+ currents (I_K-out) in mock-transfected ($n = 35$) and *ydfJ*-transfected ($n = 28$) cells with different $[K^+]_o$ and HP. Testing potential = +50 mV. $^*P < 0.05$, $^{**}P < 0.01$. **f** Summary of inward K^+ currents (I_K-in) in mock-transfected ($n = 35$) and *ydfJ*-transfected cells with different $[K^+]_o$ and HP. Testing potential = −100 mV. $^{**}P < 0.01$

transfection; 15.1 ± 1.6 pF ($n = 101$) for mock-transfected cells (empty vector), and 15.9 ± 1.8 pF ($n = 98$) for *ydfJ*-transfected HEK cells, respectively. There is no significant difference in cell capacitance between mock-transfected cells (empty vector) and *ydfJ*-transfected HEK cells. The native I_K-out in mock-transfected cells exhibited voltage-dependent increase. The average amplitude of native I_K-out was 21.9 ± 2.2 pA/pF (at +50 mV, $n = 30$) and these I_K-out showed little inactivation during 300-msec depolarization pulse (Fig. 3a). The elevation of $[K^+]_o$ from 5.4 to 40 mM significantly reduced the amplitude of native I_K-out by 25.4 ± 2.3% (at +50 mV, $n = 30$, $P < 0.05$) (Fig. 3a, b, e).

The reversal potentials of the transmembrane currents in mock-transfected cells in 5.4 mM $[K^+]_o$ were measured as −82.5 ± 7.6 mV ($n = 12$) by using classic instantaneous tail current; whereas the reversal potentials in 40 mM $[K^+]_o$ was directly measured as −29.3 ± 3.2 mV ($n = 12$) from I–V curve (Fig. 3b). The I–V relationship curves of the transmembrane currents were rightward shifted with the elevation of $[K^+]_o$ (Fig. 3b). With 40 mM $[K^+]_o$, changing holding potentials (HP) from −80 to −30 mV further decreased native I_K-out ($n = 30$, $P < 0.05$) (Fig. 3a, b, e). All these results indicated that native I_K-out of mock-transfected HEK-293 cells was carried by K^+. No native I_K-in was observed in mock-transfected cells (Fig. 3a, b, f).

On the other hand, *ydfJ* gene-transfected HEK cells had similar basal I_K-in as mock-transfected cells (Fig. 3a, c). The rise of $[K^+]_o$ to 40 mM significantly amplified I_K-in (at −100 mV) from −3.6 ± 0.3 to −30.5 ± 3.1 pA/pF, $n = 25$ ($P < 0.01$) (Fig. 3c, d, f). The elevation of $[K^+]_o$ to 40 mM reduced I_K-out (at +50 mV) by 36.6 ± 4.5% (test potential at +50 mV; $n = 25$, $P < 0.01$) (Fig. 3c–e). Changing HP from −80 to −30 mV further decreased the I_K-out by 43.7 ± 5.6% ($n = 25$, $P < 0.01$). The I_K-in were

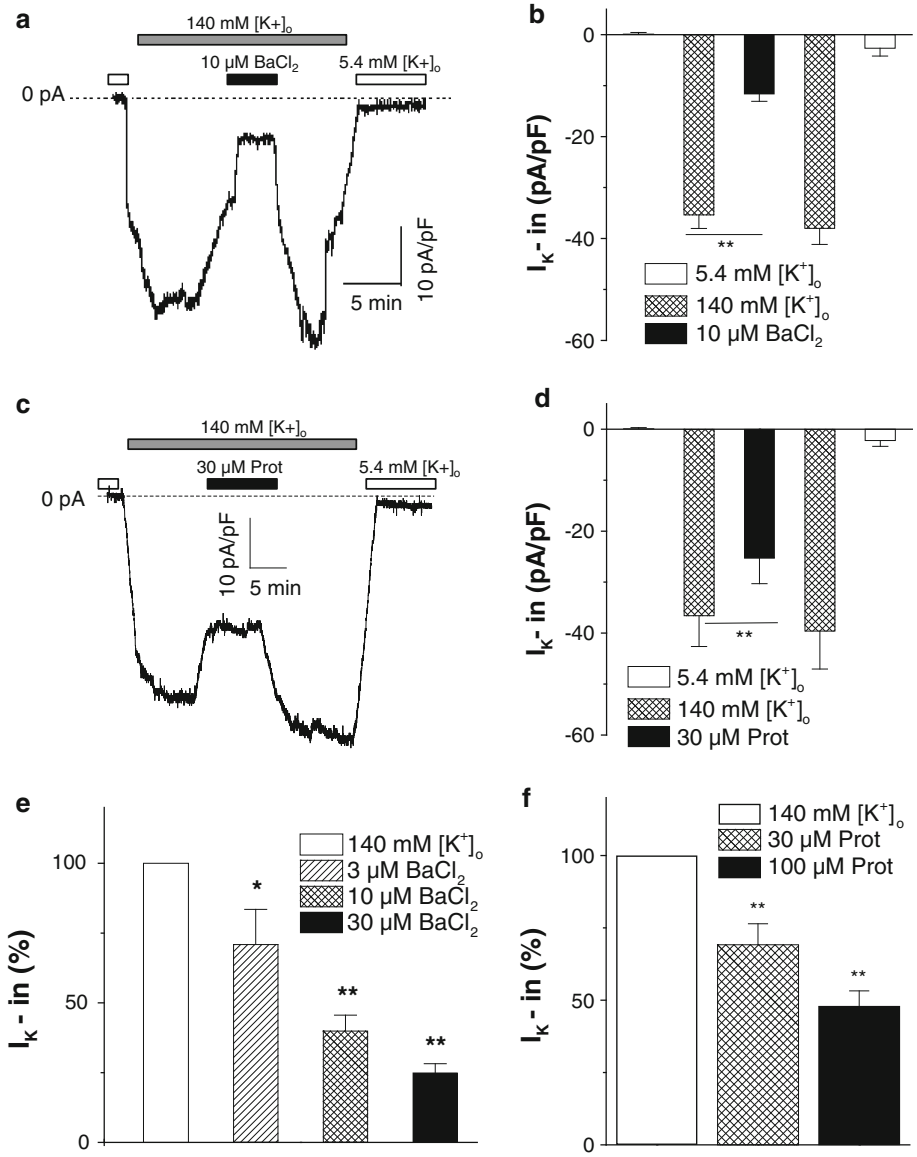

Fig. 4 Effects of $BaCl_2$ and protopine on K^+ currents in *ydfJ* gene-transfected cells. **a** Original recording with the membrane potential held at −60 mV with symmetric $[K^+]_o = 140$ mM. Bath applied $BaCl_2$ reversibly blocked the inward K^+ currents (I_K-in). **b** Summary I_K-in currents from five cells, $^{**}P < 0.01$. **c** Original recording of *ydfJ* currents. Bath applied protopine (Prot) reversibly inhibited I_K-in currents. **d** Summary effects of protopine on *ydfJ* I_K-in currents ($n = 6$). $^{**}P < 0.01$. **e** Summary inhibition of inward I_K-in by different concentration of $BaCl_2$ with the membrane potential held at −60 mV ($n = 6$). $^{*}P < 0.05$, $^{**}P < 0.01$. **f** Summary concentration-dependent inhibition of I_K-in currents by protopine ($n = 6$). $^{**}P < 0.01$

not altered by changing HP (Fig. 3c, d, f). The reversal potentials of *ydfJ*-evoked transmembrane currents were −77.65 ± 6.8 and −26.4 ± 3.0 mV with 5.4 and 40 mM $[K^+]_o$ ($n = 10$), respectively (Fig. 3d).

To amplify inward K^+ currents generated by *ydfJ* expression, membrane potential was held at −60 mV constantly and external K^+ level was changed from 5.4 to 140 mM. This shift of $[K^+]_o$ significantly increased transmembrane K^+ currents in cell line with *ydfJ* gene stable transfection from 0.2 ± 0.3 to −35.4 ± 2.6 pA/pF ($n = 6$, $P < 0.01$). This amplified inward K^+ current was reduced to −11.7 ± 1.4 pA/pF ($n = 6$, $P < 0.01$) by bath applied 10 μM $BaCl_2$. Removal of $BaCl_2$ by washout completely recovered the *ydfJ* currents from the inhibition (−38.3 ± 3.2 pA/pF, $n = 6$, $P < 0.01$) (Fig. 4a, b). Furthermore, 30 μM protopine, a nonspecific K^+ channel blocker (Song et al. 2000), reversely inhibited high K^+-evoked inward *ydfJ* currents by 30% (Fig. 4c, d). Both Ba^{2+} and protopine inhibited *ydfJ* currents in a concentration-dependent fashion (Fig. 4e, f), indicating that *ydfJ* protein encodes a Kir channel sensitive to Ba^{2+} inhibition.

To determine whether this *ydfJ* channel has the capability to form a complex with K_{ATP} channel SUR subunit, the permanent-transfection cell line with *ydfJ* gene were transiently transfected with rvSURx cDNA. K_{ATP} channel openers (diazoxide and pinacidil) or blockers (glibenclamide, giclazide, tolbutamide, PUN 37883A, and 5-HD) had no effect on the expressed *ydfJ* alone (Fig. 5a–c) or coexpressed *ydfJ*/rvSURx currents (Fig. 5d). Glibenclamide even at high dose of 100 μM was not detected to have effects on the expressed currents with *ydfJ* alone or combination with rvSURx. The amplitude of transmembrane currents in cotransfected cells with *ydfJ*/rvSUR1 or rvSUR2B was comparable to that of *ydfJ* currents (Fig. 5d). Furthermore,

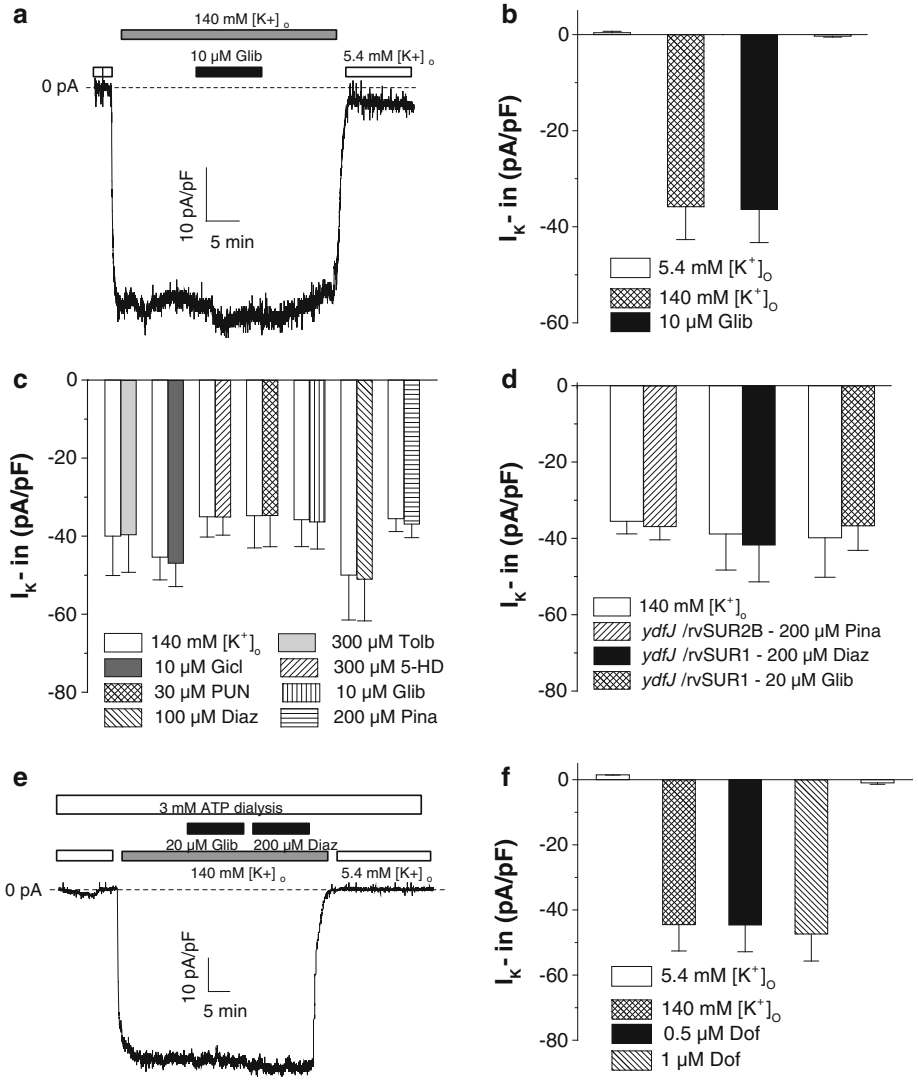

Fig. 5 Pharmacological properties of inward K^+ currents in *ydfJ* gene alone or *ydfJ*/rvSURx cotransfected cells. **a** Original recording in *ydfJ* gene permanently transfected cell with the membrane potential held constantly at −60 mV with symmetric 140 mM $[K^+]_o$ in the presence of glibenclamide (Glib). Glib at 10 μM had no effect on the inward K^+ currents (I_K-in). **b** Summary I_K-in currents from a group of six cells as in (**a**). **c** Summary effects of different K_{ATP} channel blockers and openers on I_K-in in *ydfJ*-transfected cells with symmetric 140 mM $[K^+]_o$ ($n = 9$, HP = −60 mV). **d** Summary effects of K_{ATP} channel blocker and openers on I_K-in currents in *ydfJ*/rvSUR1 or *ydfJ*/rvSUR2B cotransfected cells under the same condition as C ($n = 9$). Tolbutamide (Tolb), giclazide (Gicl), PUN37883A (PUN), diazoxide (Diaz), pinacidil (Pina). **e** Original recording of I_K-in currents in HEK-293 cells cotransfected with *ydfJ*/rvSUR2B (at HP = −60 mV). This cell was dialyzed with 3 mM ATP and perfused with 140 mM $[K^+]_o$, 20 μM Glib, and 200 μM Diaz, respectively. **f** Summary effects of a specific HERG channels blocker dofetilide (Dof) on I_K-in in *ydfJ*-transfected cells with symmetric $[K^+]_o$ ($n = 6$). HP = −60 mV

high concentration of ATP at 3–5 mM to dialyze the cells did not show any inhibitory effect on *ydfJ*/rvSURx channel activity as shown in Fig. 5e, because low concentration of ATP (0.3 mM) in pipette solution as used for recording mammalian K_{ATP} channel currents (Cao et al. 2002; Jiang et al. 2004, 2010) did not affect the amplitude of *ydfJ* current. Thus, this unknown channel is not ATP sensitive. These results ruled out the possibility that the prokaryotic *ydfJ* gene can form a complex with SUR subunits to constitute a functional mammalian K_{ATP} channel. Because *ydfJ* gene shares 12.2% sequence homology with the human ether-á-go-go-related gene (HERG), a specific HERG channels blocker dofetilide was tested its effect on *ydfJ* channel. However, we did not detect any effect of dofetilide (0.5–1 μM) on *ydfJ* currents (Fig. 5f).

Discussion

In this study, we demonstrated that *ydfJ* gene of *E. coli* K12 bacteria encodes a novel prokaryotic Kir channel and forms

a functional K^+ channel in eukaryotes. This *ydfJ* channel exhibits the following characteristics.

K^+ Selectivity

The elevation of $[K^+]_o$ from 5.4 to 40 mM mainly increased the driving force of K^+ influx and decreased the driving force of K^+ efflux, hence increasing inward current (I_K-in) and decreasing outward current (I_K-out). Because $[Cl^-]_o$ remained unchanged while $[K^+]_o$ changed, Cl^- currents does not contribute to the alteration of transmembrane current under these conditions. On the basis of Nernst Equation, the calculated K^+ equilibrium potentials at 20°C room temperature are −82.2 mV with 5.4 mM $[K^+]_o$ and −31.6 mV with 40 mM $[K^+]_o$, when $[K^+]_i$ was maintained at 140 mM. The recorded *ydfJ* currents have the approximately same reversal potentials as the theoretically calculated values, supporting the notion that *ydfJ* channel is K^+-selective.

Inward Rectification

Increasing $[K^+]_o$ from 5.4 to 40 or 140 mM enhanced the amplitude of I_K-in in *ydfJ*-transfected cells but not in mock-transfected HEK-293 cells (Fig. 3f). However, I_K-in current is voltage independent in both *ydfJ* gene- and mock-transfected cells. Changing holding potential from −80 to −30 mV decreased I_K-out of mock-transfected HEK-293 cells but this maneuver had no effect at all on the transmembrane currents in *ydfJ*-transfected cells. Although *ydfJ* gene increases endogenous I_K-out currents, the rise in $[K^+]_o$ suppresses I_K-out currents. It is noted that I_K-out in mock- and *ydfJ*-transfected cells displayed voltage-dependent outward rectification at 5.4 mM $[K^+]_o$. These results show that *ydfJ* channel is unique with inward rectified I_K-in and voltage-dependent I_K-out components.

Ba^{2+} Inhibition

Ba^{2+}, a specific inhibitor of Kir channels at 10–100 μM range, is used commonly to suppress K^+ conductance as a result of its tight binding within the channel pore from extracellular side (Reimann and Ashcroft 1999; Sun et al. 2006). Our result demonstrated that bath applied Ba^{2+} at 10–30 μM inhibited reversibly *ydfJ* currents in a dose-dependent fashion, supporting further that *ydfJ*-encoded protein is a Kir channel.

Differences from K_{ATP} Channel Subunits

It is known that SUR1 subunit increases the amplitude of K_{ATP} currents in Kir6.1 cotransfected HEK-293 cells and tolbutamide at 0.5 mM significantly suppressed coexpressed Kir6.1/SUR1 currents, rather than Kir6.1 alone-generated currents (Ammala et al. 1996). However, *ydfJ*/rvSUR1 or *ydfJ*/rvSUR2B currents in HEK-293 cells had comparable amplitude with that of *ydfJ* currents, indicating that SUR1 or SUR2B does not couple *ydfJ* protein to form the functional K_{ATP} channel complex. Furthermore, neither *ydfJ* currents nor *ydfJ*/rvSUR1 or rvSUR2B currents in HEK-293 cells were sensitive to ATP and K_{ATP} channel openers and/or blockers, confirming that *ydfJ* protein was not a component of K_{ATP} channel complex. Protopine inhibits cardiac K^+ currents, including inward rectifier and delayed rectifier (Song et al. 2000). When rvKir6.1 alone is expressed in HEK-293 cells, protopine has no effect on this channel current (Jiang et al. 2004). However, *ydfJ* channel is inhibited reversibly by protopine. This suggests that *ydfJ* is unlikely to function as a K_{ATP} channel subunit.

Difference from HERG Channels

High concentrations of dofetilide have been used to block HERG channels with IC_{50} of 0.2–0.5 μM (Dong et al. 2004; Kiehn et al. 1995). However, *ydfJ* current in this study was not inhibited by dofetilide even at 0.5–1 μM. This indicates that *ydfJ* channel is different from HERG channels. All aforementioned characteristics indicate that *ydfJ* gene encodes a novel Kir channel protein, which is different from classical K_{ATP} channels or HERG channel in mammalian cells.

As the name implies, *E. coli* K12 contains the capsular (K) antigen 12. This strain of *E. coli* is a friendly bacterium as it can produce vitamins K that we require (Conly and Stein 1994; Kindberg et al. 1987). *E. coli* K12 has been developed as a key research tool for studying basic biology processes because this commensal microbe is safe to handle without virulence factors. Furthermore, *E. coli* K12 strain is the frequently used earliest organism as a good candidate for the whole genome sequencing and biochemical genetics (Blattner 1983; Blattner et al. 1997). *E. coli* K12 has a single circular chromosome with 4288 protein-coding genes, however, of which 38% have no attributed function. We screened *E. coli* K12 genome with conserved TM1–H5–TM2 region of rvKir6.1/rvKir6.2 and found three genes (*ydfJ*, *ydeE*, and *ybbW*) with highest percentage of identity to rvKir6.1/rvKir6.2. The function of these three genes has not been experimentally clarified. In this study, we cloned *ydfJ* gene and heterologously expressed it in mammalian cells. Although prokaryotic Kir channels have proven particularly informative of the structure of the related mammalian Kir channel family (Loukin et al. 2005), our study presents original evidence that a prokaryotic gene is capable of forming a functional K^+ channels in mammalian cell. By doing so, we

demonstrated that the comparison of bacterial genomes with known eukaryotic channel gene sequence would provide clues for the structure and functions of unknown ion channels in both prokaryotic and eukaryotic cells. Our strategy starts with the bioinformatic approach to search known bacterial genomes for desired channel genes with some degree of sequence homologous with mammalian Kir6.1/Kir6.2 channels by using Basic Local Alignment Search Tool (BLAST). The second step was to retrieve the selected gene (*ydfJ*) through PCR from the genomic DNA of the original candidate organism (*E. coli* K12), and then clone and sequence the candidate bacterial gene by transforming it into *E. coli* competence cells. Thirdly, we expressed heterologously the cloned bacterial gene in mammalian expression system. Finally, we characterize the biophysical and pharmacological properties of the expressed channel protein. Through this strategy, our study demonstrated that the prokaryotic *ydfJ* gene can produce a functional K^+ conduit in eukaryotic cells as the corresponding K^+ currents were detected by using the patch clamp technique.

The crystal structures of KirBac, a family of prokaryotic genes homologous to eukaryotic Kir channels, including KirBac1.1, KirBac3.1, and KirBac3.1/Kir3.1 chimera, have been revealed in several molecular modeling studies (Kuo et al. 2003, 2005a, b Nishida et al. 2007). Until recently electrophysiological evidence (Cheng et al. 2009) has not been available to substantiate these computational studies, and functional studies of KirBac1.1 have been limited to $^{86}Rb^+$ flux assay of proteoliposomes as well as bacteria or yeast complementation screenings (Enkvetchakul and Nichols 2003; Sun et al. 2006). The only voltage clamp analysis reported was on recombinant channel activity in excised membrane patches from giant liposomes after the full-length His-tagged KirBac1.1 protein were expressed in *E. coli* BL21, DE3 strain (Cheng et al. 2009). The authors showed that KirBac1.1 generates functional K^+-selective channels that exhibits the same key features of inward rectification found in eukaryotic Kir channels. There are major differences between *ydfJ* channel and KirBac1.1 channel. (1) Different amino acid sequence and homology: *ydfJ* protein has 427 amino acids from *E. coli* K12, while KirBac1.1 has 333 amino acids from *Burkholderia pseudomallei.* In terms of homogeneity of TM1–H5–TM2 sequence to Kir6.1 and Kir6.2, *ydfJ* has 12.7 and 15.7% homology, respectively; whereas KirBac1.1 has 19.6 and 22.7% homology, respectively (Table 1). (2) Formation of functional channels in different expression systems: *ydfJ* gene is transfected into mammalian expression system and forms functional K^+ channel in HEK-293 cell; whereas KirBac1.1 protein is reconstituted in artificial liposomes. (3) Different Ba^{2+} sensitivity: Inwardly rectified *ydfJ* channels are significantly inhibited dose-dependently by micromolar Ba^{2+}. On the other hand, millimolar Ba^{2+} only blocked outward KirBac1.1 currents but had no effect on inward KirBac1.1 current.

Classical mammalian K^+ channels share a highly conserved signature sequence with 6 residues of "TTV(I/A)GY(F)G" (Heginbotham et al. 1994). The functional relevance of this signature sequence may be the determination of K^+ selectivity of mammalian K^+ channels (Heginbotham et al. 1994). However, K^+ selectivity can be abolished by mutations outside the K^+ channel signature sequence (Yi et al. 2001). Recently published paper (Derebe et al. 2011) demonstrated that the number of contiguous ion binding sites in tetrameric cation channels is the key determinant of the channel's selectivity properties and the presence of four sites in K^+ channels is essential for highly selective and efficient permeation of K^+ ions. In the place of the classical signature sequence for mammalian K^+ channels, *ydfJ* gene has 6 different residues of "QGLGAG." Still, *ydfJ*-coded K^+ channels possess K^+ selectivity. It is speculated that the whole signature sequence of mammalian K^+ channel may not be as critical as the conserved triplet GXG (X being any amino acid residue) for K^+ selectivity. Although *ydfJ* gene was originally classified as a member of major facilitator superfamily (MFS) Permeases of *Escherichia coli* K12 family, the functional *ydfJ*-encoded protein has never been reported. In fact, the belonging of *ydfJ gene* to MFS family is doubted. *ydfJ-coded* protein lacks a uniform topology of 12 transmembrane α-helices connected by hydrophilic loops that almost all MSF proteins possess (Pao et al. 1998). *ydfJ* protein also does not have the conserved signature sequences "DRXXRR" (D-aspartic acid; R, arginine) for MFS family in the loops between TM2 to TM3 (Maiden et al. 1987). Together with its property as a functional K^+ channel, *ydfJ* protein is closer to a mammalian K^+ channel than to a MFS transporter.

In summary, *ydfJ* gene from *E. coli* K12 encoded a novel inwardly rectifying K^+-selective channel protein. For the first time, a prokaryotic gene was heterologously expressed in mammalian HEK-293 cells and formed a functional K^+ channel. The strategy of homologous search for unknown bacterial ion channels on the basis of known eukaryotic ion channel genes (TM1-P-TM2 topology and K^+ selectivity filter sequence of Kir6.1 and Kir6.2) may facilitate discovering other unknown functional ion channels or transport proteins and revealing their structure-function relationship. Thus, the identification of a novel *ydfJ*-encoded K^+ channel expands our understanding of the compositional makeup of K channel families. At this moment, whether this new bacterial-originated ion channels are expressed in mammalian cells and affect their physiological function is not clear. Further characterization of the expression pattern and intensity of this novel channel in mammalian cells under different conditions may help

link specific cellular functions to this novel channel. Rigorous sequence alignments and transmembrane predictions of this new channel may be used to assign family members and evolutionary relatedness.

Acknowledgments This study was supported by an operating grant from Canadian Institutes of Health Research. G. Tang received a postdoctoral fellowship from the Heart and Stroke Foundation of Canada.

References

Ammala C, Moorhouse A, Gribble F, Ashfield R, Proks P, Smith PA, Sakura H, Coles B, Ashcroft SH, Ashcroft FM (1996) Promiscuous coupling between the sulphonylurea receptor and inwardly rectifying potassium channels. Nature 379:545–548

Ashcroft FM (2005) ATP-sensitive potassium channelopathies: focus on insulin secretion. J Clin Invest 115:2047–2058

Bichet D, Haass FA, Jan LY (2003) Merging functional studies with structures of inward-rectifier K^+ channels. Nat Rev Neurosci 4:957–967

Blattner FR (1983) Biological frontiers. Science 222:719–720

Blattner FR, Plunkett G III, Bloch CA, Perna NT, Burland V, Riley M, Collado-Vides J, Glasner JD, Rode CK, Mayhew GF, Gregor J, Wayne Davis N, Kirkpatrick HA, Goeden MA, Rose DJ, Mau B, Shao Y (1997) The complete genome sequence of *Escherichia coli* K-12. Science 277:1453–1462

Cao K, Tang G, Hu D, Wang R (2002) Molecular basis of ATP-sensitive K^+ channels in rat vascular smooth muscles. Biochem Biophys Res Commun 296:463–469

Cheng WW, Enkvetchakul D, Nichols CG (2009) KirBac1.1: it's an inward rectifying potassium channel. J Gen Physiol 133:295–305

Conly J, Stein K (1994) Reduction of vitamin K2 concentrations in human liver associated with the use of broad spectrum antimicrobials. Clin Invest Med 17:531–539

Derebe GM, Sauer DB, Zeng W, Alam A, Shi N, Jiang Y (2011) Tuning the ion selectivity of tetrameric cation channels by changing the number of the ion binding sites. Proc Natl Acad Sci USA 108:598–602

Dobrindt U (2005) Patho-Genomics of *Escherichia coli*. Int J Med Microbiol 295:357–371

Dong DL, Li Z, Wang HZ, Du ZM, Song WH, Yang BF (2004) Acidification alters antiarrhythmic drug blockade of the ether-á-go-go-related gene (HERG) channels. Basic Clin Pharmacol Toxicol 94:209–212

Durell SR, Guy HR (2001) A family of putative Kir potassium channels in prokaryotes. BMC Evol Biol 1:14

Enkvetchakul D, Nichols CG (2003) Gating mechanism of K_{ATP} channels: function fits form. J Gen Physiol 122:471–480

Enkvetchakul D, Bhattacharyya J, Jeliazkova I, Groesbeck DK, Cukras CA, Nichols CG (2005a) Functional characterization of a prokaryotic Kir channel. J Biol Chem 279:47076–47080

Enkvetchakul D, Jeliazkova I, Nichols CG (2005b) Direct modulation of Kir channel gating by membrane phosphatidylinositol 4,5-bisphosphate. J Biol Chem 280:35785–35788

Hebert SC (2003) Bartter syndrome. Curr Opin Nephrol Hypertens 12:527–532

Heginbotham L, Lu Z, Abramson T, MacKinnon R (1994) Mutations in the K^+ channel signature sequence. Biophys J 66:1061–1067

Higgins DG, Sharp PM (1988) CLUSTAL: a package for performing multiple sequence alignment on a microcomputer. Gene 73:237–244

Jiang Y, Lee A, Chen J, Cadene M, Chait BT, MacKinnon R (2002) Crystal structure and mechanism of a calcium-gated potassium channel. Nature 417:515–522

Jiang B, Cao K, Wang R (2004) Inhibitory effect of protopine on K_{ATP} channel subunits expressed in HEK-293 cells. Eur J Pharmacol 506:93–100

Jiang B, Tang G, Cao K, Wu L, Wang R (2010) Molecular mechanism for H_2S-induced activation of K_{ATP} channels. Antioxid Redox Signal 12:1167–1178

Kiehn J, Wible B, Ficker E, Taglialatela M, Brown AM (1995) Cloned human inward rectifier K^+ channel as a target for class III methanesulfonanilides. Circ Res 77:1151–1155

Kindberg C, Suttie JW, Uchida K, Hirauchi K, Nakao H (1987) Menaquinone production and utilization in germ-free rats after inoculation with specific organisms. J Nutr 117:1032–1035

Kowalski A, Martinac B (2005) Ion channels and their eukaryotic homologs. ASM, Washington, DC

Kung C, Blount P (2004) Channels in microbes: so many holes to fill. Mol Microbiol 53:373–380

Kuo A, Gulbis JM, Antcliff JF, Rahman T, Lowe ED, Zimmer J, Cuthbertson J, Ashcroft FM, Ezaki T, Doyle DA (2003) Crystal structure of the potassium channel KirBac1.1 in the closed state. Science 300(5627):1922–1926

Kuo A, Domene C, Johnson LN, Doyle DA, Vénien-Bryan C (2005a) Two different conformational states of the KirBac3.1 potassium channel revealed by electron crystallography. Structure 13: 1463–1472

Kuo MM, Haynes WJ, Loukin SH, Kung C, Saimi Y (2005b) Prokaryotic K^+ channels: from crystal structures to diversity. FEMS Microbiol Rev 29:961–985

Loukin SH, Kuo MM, Zhou XL (2005) Microbial K^+ channels. J Gen Physiol 125:521–527

Loussouarn G, Rose T, Nichols CG (2002) Structural basis of inward rectifying potassium channel gating. Treands Cardiovasc Med 12:253–258

Maiden MC, Davis EO, Baldwin SA, Moore DC, Henderson PJ (1987) Mammalian and bacterial sugar transport proteins are homologous. Nature 325(6105):641–643

Nishida M, Cadene M, Chait BT, MacKinnon R (2007) Crystal structure of a Kir3.1-prokaryotic Kir channel chimera. EMBO J 26:4005–4015

Pao SS, Paulsen IT, Saier MH Jr (1998) Major facilitator superfamily. Microbiol Mol Biol Rev 62:1–34

Plaster NM, Tawil R, Tristani-Firouzi M, Canun S, Bendahhou S, Tsunoda A, Donaldson MR, Iannaccone ST, Brunt E, Barohn R, Clark J, Deymeer F, George AL Jr, Fish FA, Hahn A, Nitu A, Ozdemir C, Serdaroglu P, Subramony SH, Wolfe G, Fu YH, Ptacek LJ (2001) Mutations in Kir2.1 cause the developmental and episodic electrical phenotypes of Andersen's syndrome. Cell 105:511–519

Reimann F, Ashcroft FM (1999) Inwardly rectifying potassium channels. Curr Opin Cell Biol 11:503–508

Ruta V, Jiang Y, Lee A, Chen J, MacKinnon R (2003) Functional analysis of an archaebacterial voltage-dependent K^+ channel. Nature 422(6928):180–185

Seino S (1999) ATP-sensitive potassium channels: a model of heteromultimeric potassium channel/receptor assemblies. Annu Rev Physiol 61:337–362

Song LS, Ren GJ, Chen ZL, Chen ZH, Zhou ZN, Cheng H (2000) Electrophysiological effects of protopine in cardiac myocytes: inhibition of multiple cation channel currents. Br J Pharmacol 129:893–900

Sun S, Gan JH, Paynter JJ, Tucker SJ (2006) Cloning and functional characterization of a superfamily of microbial inwardly rectifying potassium channels. Physiol Genomics 26:1–7

Tang G, Wu L, Liang W, Wang R (2005) Direct stimulation of K_{ATP} channels by exogenous and endogenous hydrogen sulfide in vascular smooth muscle cells. Mol Pharmacol 68:1757–1764

Wu L, Cao K, Lu Y, Wang R (2002) Different mechanisms underlying the stimulation of K_{Ca} by nitric channels oxide and carbon monoxide. J Clin Invest 110:691–700

Yi BA, Lin YF, Jan YN, Jan LY (2001) Yeast screen for constitutively active mutant G protein-activated potassium channels. Neuron 29:657–667